

Review

Toward Scalable Liquid-Phase Synthesis of Sulfide Solid Electrolytes for All-Solid-State Batteries

Hirotada Gamo ^{1,*†}, Atsushi Nagai ² and Atsunori Matsuda ^{1,*} 

¹ Department of Electrical and Electronic Information Engineering, Toyohashi University of Technology, 1-1 Hibarigaoka, Toyohashi 441-8580, Aichi, Japan

² Next-Generation Energy Systems Group, Centre of Excellence ENSEMBLE3 sp. z o.o., Wolczynska 133, 01-919 Warsaw, Poland; atsushi.nagai@ensemble3.eu

* Correspondence: h.gmaou@aist.go.jp (H.G.); matsuda@ee.tut.ac.jp (A.M.)

† Current Address: Research Institute of Electrochemical Energy, Department of Energy and Environment, National Institute of Advanced Industrial Science and Technology (AIST), 1-8-31, Ikeda 563-8577, Osaka, Japan.

Abstract: All-solid-state batteries (ASSBs) are promising to be next-generation battery that provides high energy density and intrinsic safety. Research in the field of ASSBs has so far focused on the development of highly conductive solid electrolytes (SEs). The commercialization of ASSBs requires well-established large-scale manufacturing for sulfide SEs with high ionic conductivity. However, the synthesis for sulfide SEs remains at the laboratory scale with limited scalability owing to their air sensitivity. The liquid-phase synthesis would be an economically viable manufacturing technology for sulfide SEs. Herein, we review a chemical perspective in liquid-phase synthesis that offers high scalability, low cost, and high reaction kinetics. This review provides a guideline for desirable solvent selection based on the solubility and polarity characterized by the donor number and dielectric permittivity of solvents. Additionally, we offer a deeper understanding of the recent works on scalable liquid-phase synthesis using solubilizers and reactant agents. We present an outlook on a universal liquid-phase synthesis of sulfide SEs toward the commercialization of sulfide-based ASSBs.



Citation: Gamo, H.; Nagai, A.; Matsuda, A. Toward Scalable Liquid-Phase Synthesis of Sulfide Solid Electrolytes for All-Solid-State Batteries. *Batteries* **2023**, *9*, 355.
<https://doi.org/10.3390/batteries9070355>

Academic Editors: Jae-won Lee

Received: 27 May 2023

Revised: 19 June 2023

Accepted: 30 June 2023

Published: 4 July 2023



Copyright: © 2023 by the authors. Licensee MDPI, Basel, Switzerland. This article is an open access article distributed under the terms and conditions of the Creative Commons Attribution (CC BY) license (<https://creativecommons.org/licenses/by/4.0/>).

1. Introduction

Lithium-ion batteries (LIBs) are attracting attention as a power source for electric vehicles (EVs) [1]. EV sales are expected to grow tenfold by the end of this decade, even though they were just 2–3% of total passenger vehicle sales in 2020 [2]. However, traditional LIBs with flammable organic liquid electrolytes have safety issues, such as leakage and ignition. These issues remain critical obstacles that hinder the market adoption of LIBs in the EV field [3]. All-solid-state lithium-ion batteries (ASLBs) with non-flammable inorganic solid electrolytes (SEs) offer inherently higher safety [3,4]. Inorganic SEs are crucial for the development of ASLBs that meet the demanding requirements of the EV sector for safer and greater batteries. Extensive material exploration to date has led to the discovery of highly conducting crystalline $\text{Li}_7\text{P}_3\text{S}_{11}$ and $\text{Li}_{10}\text{GeP}_2\text{S}_{12}$, which exhibit an ionic conductivity in the order of $10^{-2} \text{ S cm}^{-1}$ at room temperature, comparable with those of organic liquid electrolytes [5,6]. This discovery has largely advanced the application of sulfide-based ASLBs [7,8]. Recent research has focused on the material design of a family of argyrodite-type SEs with high ionic conductivity and moderate electrochemical stability. Sulfide SEs are generally synthesized by the solid-phase method using quartz ampoules or the mechanochemical method using ball-milling. These synthetic techniques are used on a laboratory scale for the discovery and design of novel materials. The synthesis is commonly performed in a glove box under an inert atmosphere because sulfide SEs and

their raw materials react with moisture in the air to release toxic H₂S gas. Given the low scalability of both synthetic methods, the scientific community developing sulfide-based ASLBs is currently interested in manufacturing technologies involving a level of practical application [9].

The liquid-phase method would be an economically viable technology for ASLB manufacturing [10,11]. However, the liquid-phase synthesis of sulfide SEs is not described by only the simple chemical reactions of raw materials [12]. The liquid-phase synthesis involves complex interactions influenced by a solvent coordination bond, competition between the solvent and chemical species, and other factors [13]. Such interactions are significantly influenced by raw materials and their compositions, which determine the solubility and reactivity in the liquid-phase synthesis of sulfide SEs. The reaction mechanism, solubility, and reactivity of Li₂S-P₂S₅ compounds (common sulfide SEs) in solvents are becoming evident, but there is sparse understanding of these chemical perspectives in the other family of sulfide SEs, which consists of SiS₂ and GeS₂ in solvents. In addition, the reaction mechanism of sulfide SEs doped with lithium halides, which are often introduced to improve ionic conductivity and electrochemical stability, in solvents is unclear because of the coordination structure altered by the presence of the halide ions. The liquid-phase synthesis involves several difficulties: estimation of increasing increments for the nucleophilic and electrophilic contributions, respectively; the choice of optimal empirical parameters for the nucleophilic and the electrophilic functions; and the understanding of the reaction mechanism [13–15]. Therefore, the liquid-phase synthesis of sulfide SEs has been advanced by an empirical approach so far [15–18]. This review aims to discuss the chemical perspective in the liquid-phase synthesis for sulfide SEs and provide a design guideline for the liquid-phase synthesis that realizes the high scalability, low cost, and short reaction processing time.

2. The Liquid-Phase Synthesis Method

In the liquid-phase synthesis, sulfide SEs are generally synthesized through a chemical reaction in solvents, solvent removal, and the crystallization process. This synthesis method is classified into suspension and solution synthesis, depending on the state of the solution in the reaction process, as shown in Figure 1. The state during the reaction process is determined by the properties of the solvent.

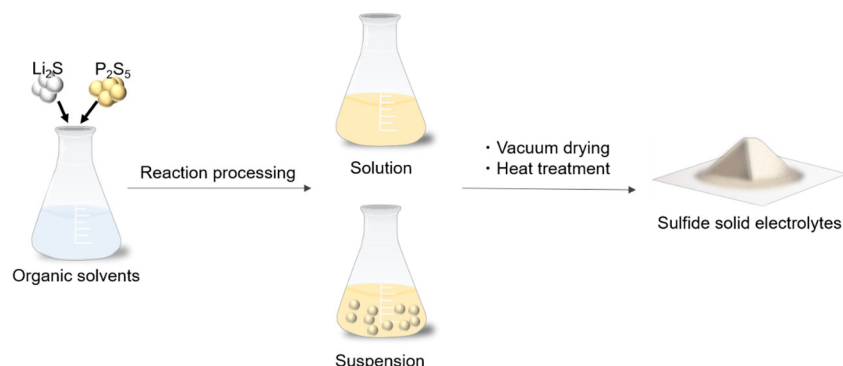


Figure 1. Schematic of the liquid-phase synthesis for sulfide-based solid electrolytes.

2.1. Suspension Synthesis

In suspension synthesis, precursor suspensions are obtained through the chemical reactions of raw materials in a solvent with moderate solubility [10]. The synthesis of sulfide SEs via suspension is summarized in Table 1. Li₂S-P₂S₅ systems are generally synthesized via the suspension because of their incomplete dissolution in most aprotic polar solvents. Liang et al. first synthesized nanoporous β -Li₃PS₄ via the suspension process using tetrahydrofuran (THF) [19]. A mixture of Li₂S and P₄S₁₀ (commonly referred to as P₂S₅ in the literature) is reacted overnight in THF to generate an Li₃PS₄·3THF complex. This

compound releases THF molecules under a vacuum at 80 °C, followed by heating at 140 °C under a vacuum to produce the β -Li₃PS₄ with an ionic conductivity of 7.4×10^{-5} S cm⁻¹ at room temperature. Subsequent research found that 1,2-dimethoxyethane (DME) [20], acetonitrile (ACN) [15,16], ethyl acetate (EA) [21,22], ethyl propionate (EP) [23,24], pyridine [25,26], and anisole [27] are also used as an effective reaction solvent for the suspension synthesis owing to their moderate solubility and reactivity. Lithium sulfide and P₂S₅ reactants are individually insoluble in most aprotic polar solvents, but form highly soluble solvate lithium thiophosphates at a 1:1 molar ratio of Li₂S and P₂S₅ [28]. The intermediate reacts with Li₂S to generate Li₃PS₄ precursors. The reaction from insoluble Li₂S to insoluble Li₃PS₄ involves a long processing time (1–3 days) because of the sluggish reaction kinetics. The suspension synthesis of Li₇P₃S₁₁ and Li₇P₂S₈I involves the rate-limiting process of the Li₃PS₄ precursor formation [29–31]. This process involves the formation of heterogeneous precursors, which may increase the engineering cost of ASLB manufacturing, particularly for large-scale manufacturing. On the other hand, giving additional energy by mechanical [23], super sonication [32], and microwave [27] treatments allows us to boost the reaction kinetics and reduce the processing time. The liquid-phase synthesis assisted by the mechanical treatment provided the rapid synthesis of the Li₃PS₄ SEs with an ionic conductivity over 10⁻⁴ S cm⁻¹ at room temperature [33]. Amorphous Li₃PS₄ prepared by the mechanochemical reaction shows higher ionic conductivity than the crystalline β -phase [34]. Thus, in the liquid-phase synthesis, the solvent removal process should be conducted at a lower temperature than the crystallization temperature of β -Li₃PS₄ to achieve high ionic conductivity. The evaporation temperature of a coordinated solvent depends on the strength of the coordination bond between the solvent and intermediate molecular complex, which is determined by the polarity of the solvent. In the liquid-phase synthesis of Li₃PS₄ via acetate solvent systems, solvents with lower polarity resulted in a lower temperature of the solvent removal [22]. Li₃PS₄ synthesized using acetate solvents with lower polarity showed higher ionic conductivity because of the formation of low crystallinity Li₃PS₄, even after the solvent removal.

Table 1. Synthesis of sulfide SEs via suspension.

Product	Treatment	Solvent	Reaction Time (h)	Ionic Conductivity (mS cm ⁻¹)	Reference
Li ₃ PS ₄	Stirring	THF	12	0.074	[19]
Li ₃ PS ₄	Stirring	ACN	48	0.12	[14]
Li ₃ PS ₄	Shaking	EP	6	0.20	[33]
Li ₇ P ₃ S ₁₁	Stirring	DME	72	0.27	[20]
Li ₇ P ₃ S ₁₁	Stirring	ACN	24	1.5	[35]
Li ₇ P ₃ S ₁₁	Sonication	ACN	0.5	1.0	[32]
Li ₇ P ₃ S ₁₁	Microwave	anisole	0.5	0.13	[27]
Li ₇ P ₂ S ₈ I	Stirring	ACN	36	0.63	[31]
Li ₇ P ₂ S ₈ I	Shaking	EP	6	0.34	[23]
Li ₇ P ₂ S ₈ I	Shaking	EP	1	1.0	[36]
Li ₆ PS ₅ Cl	Stirring	THF+EtOH	36	2.4	[37]
Li ₆ PS ₅ Cl	Stirring	ACN+PTH	24	2.8	[38]

In the suspension synthesis of Li₆PS₅Cl, alcohol solvents are used as effective reaction mediators. For instance, ethanol (EtOH) solvent shows an extremely high solubility against Li₂S and P₂S₅, but causes a substitution reaction between the O atom in the solvent and the S atom in the P₂S₅ molecule. Despite this limitation, the Li₆PS₅Cl precursor was synthesized by the reaction of the Li₃PS₄ THF complex precursor, Li₂S, and LiCl in an alcohol solvent [37,39]. We believe that this is because the PS₄³⁻ anion unit is protected from EtOH by steric hindrance from THF coordinated to 3Li⁺-PS₄³⁻. The Li₆PS₅Cl SEs did not return to their original argyrodite structure after dissolving in EtOH and heating again [40]. This should be derived from the severe decomposition of PS₄³⁻ by EtOH. The decomposition of the Li₆PS₅Cl by EtOH can be minimized by decreasing the exposure time

to EtOH [41,42]. Considering the side reactions caused by EtOH, a synthesis method using an ACN/1-propanethiol (PTH) solvent was developed [38]. The Li₆PS₅Cl SEs synthesized using the THF/EtOH solvent contained an Li₃PO₄ crystal phase as a secondary phase (see Figure 2a). Even Li₆PS₅Cl synthesized using THF/PTH formed oxides in the final product, which originated from the ring-opening reaction of THF solvent caused by the nucleophilic attack of the dissociated Cl ions and the $-S^-$ anion of PTH. On the other hand, highly pure Li₆PS₅Cl SEs without Li₃PO₄ were successfully synthesized in an oxygen-free system using ACN/PTH solvent (Figure 2b). Additionally, Li₆PS₅Cl SEs with relatively high purity were synthesized using only the THF single solvent by employing a heat treatment to fully react the raw materials [43].

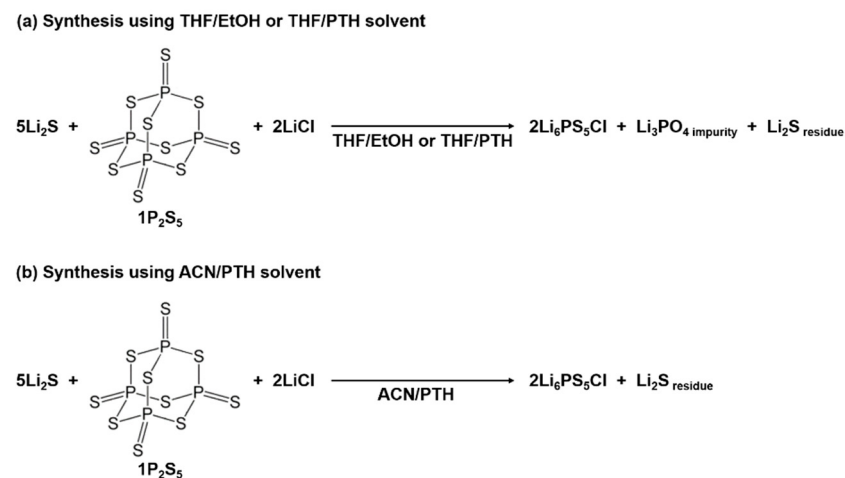


Figure 2. Schematics of the wet-chemical synthesis of Li₆PS₅Cl SEs in (a) THF/EtOH or THF/PTH and (b) ACN/PTH solvents.

2.2. Solution Synthesis

The solution synthesis involves the formation of a homogeneous precursor solution in an organic solvent with high solubility. Hence, the solution synthesis method provides faster reaction kinetics in comparison with suspension synthesis. Table 2 summarizes the synthesis of sulfide SEs via the solution. Recent works reported that ethylene diamine (EDA) and EA dissolve 75Li₂S·25P₂S₅ [44,45] and 70Li₂S·30P₂S₅ (mol%) [21], respectively. It should be noted that the solubility of the solvent may be influenced by the presence of slight moisture in the solvent. In addition, polar hydrophilic protonic solvents, such as dimethylformamide (DMF) and 1-methyl-2-pyrrolidone (NMP), exhibit high solubility against Li₂S and P₂S₅ [46]. However, their use is limited because of their high basicity, which leads to the decomposition of anion units in intermediate molecular complexes [17,46,47]. Thiol solvents were found to be effective solvents for the solution synthesis of sulfide SEs [48,49]. Thiol solvents exhibit desirable properties, such as high polarity, high solubility, moderately low boiling point, and no side reactions with the raw materials and intermediates. A mixed solvent containing thiol solvent and EDA is a useful reaction solvent for a broad range of sulfide SEs, including Li₆PS₅Cl and Li₁₀Ge₂PS₁₂ [49]. With the use of ethanedithiol (EDT) solvent, carbonized solvent molecules remained in the sulfide SEs after heat treatment. This should be ascribed to the strong coordination bonds between the solvent molecules and solutes. The presence of residual solvent molecules led to high electronic conductivity of the SEs, which negatively affected their performance as an electrolyte for ASLBs. Generally, there is a relationship between the strength of the coordination bonds with solvent molecules and the evaporation temperature of the coordinated solvent. The use of the highly polar solvent may increase the industrial cost due to the large energy consumption in the solvent removal process. Taking this into consideration, an ideal manufacturing process would involve the complete dissolution of the precursor and precipitation of the

final product, thereby improving yield, reducing production costs, and minimizing waste and solvent removal.

Table 2. Synthesis of sulfide SEs via solution.

Product	Treatment	Solvent	Reaction Time (h)	Ionic Conductivity (mS cm^{-1})	Reference
Li_3PS_4	Stirring	EDA	3	2.3×10^{-3}	[44]
$\text{Li}_7\text{P}_3\text{S}_{11}$	Stirring	EA	2	0.12	[21]
$\text{Li}_{6-x}\text{PS}_{5-x}\text{Cl}_{1+x}$ ($0 \leq x \leq 0.5$)	Stirring	EDA	—	2.9	[25]
$\text{Li}_{10}\text{Ge}_2\text{PS}_{12}$	Stirring	EDA+ET	3	1.2	[49]

3. Solvent Selection

The solvent selection in the liquid-phase synthesis is a critical consideration, taking into account factors such as solvent polarity, solubility of reactants, products, and intermediates, solvent removal processes, and industrial concerns [12]. This review focuses on the topics of polarity and solubility. The polarity of organic solvents varies the bond properties in the intermediate molecular complexes. The extent of polarization induced by a given bond relies on the strength of the coordination bonds with the nucleophile and/or electrophile. The stronger the coordination interaction, the greater the induced polarization. The reaction between Li_2S and P_2S_5 is initiated by the dissociation reaction of the P_2S_5 through nucleophilic attack by the electron donor [50]. Therefore, the introduction of empirical functional parameters related to nucleophilic property is important for the effective synthesis of sulfide SEs via the liquid phase. Donor number (DN) and dielectric permittivity are commonly used as empirical parameters to quantify polarity. Table 3 summarizes the DN, dielectric permittivity, and boiling point of various solvents.

Table 3. Functional parameter and physical properties of various solvents [13,51].

Solvent	Donor Number [$\text{kcal}\cdot\text{mol}^{-1}$]	Dielectric Permittivity	Boiling Point [$^{\circ}\text{C}$]
1,4-dioxan	15	2.2	101
Carbon sulfide	2	2.63	46
Anisole	9	4	154
Tetrahydropyran	22	5.5	88
Ethyl acetate	17	6	77
1,2-Dimethoxyethane	24	7.2	83
Tetrahydrofuran	20	7.6	66
Pyridine	33	12	115
Ethylene diamine	55	14	116
Ethanol	32	19	78
Dimethylformamide	27	36	153
Acetonitrile	14	38	82

3.1. Donor Number

The DN is defined as the negative enthalpy for the reaction of complexation with SbCl_5 in a highly diluted solution of dichloroethane. The concept of DN was proposed to express quantitatively the Lewis basicity of solvents. Aprotic solvents, in general, exhibit poor accepter properties, and their DN values are related to the extent of charge transfer associated with ion solvation [13]. Hence, the DN of a solvent serves as an indicator of its reactivity in liquid-phase synthesis. Previous studies reported that organic solvents with DN higher than 14 kcal mol^{-1} were unsuitable for solution processing of Li_3PS_4 SEs because of their decomposition caused by nucleophilic attacks [18]. While THF has 20 kcal mol^{-1} of DN, it is often used for the solution processing of sulfide SEs [40,43]. However, the guideline for solvent selection is not contingent on DN indicators only. EDA

solvent shows the highest DN among the solvents listed in Table 3. The EDA with high DN acts as a strong nucleophilic agent, breaking the P-S bond in P_2S_5 and facilitating the complete dissolution of P_2S_5 [44]. The 75Li₂S 25P₂S₅ solution in EDA contains various units such as PS_4^{3-} , $P_2S_6^{4-}$, $P_2S_6^{2-}$, and PS_3^- , which convert into β -Li₃PS₄ consisting exclusively of PS_4^{3-} units after heat-treatment at 200 °C under vacuum.

3.2. Dielectric Permittivity

Dielectric permittivity is an important indicator for evaluating the polarity of solvents and determining their reactivity in wet-chemical synthesis. It was found that the dielectronic permittivity of solvents used in the synthesis relates to the ionic conductivity of Li₇P₃S₁₁ prepared by the suspension synthesis [15]. Figure 3a illustrates the correlation between the ionic conductivity of Li₇P₃S₁₁ at room temperature and the dielectronic permittivity of the used organic solvents. Higher dielectronic permittivity of the solvents leads to increased ionic conductivity in the Li₇P₃S₁₁. There is no relationship between the DN of the solvent and the ionic conductivity of Li₇P₃S₁₁ SEs. Figure 3b displays differential thermal curves of Li₇P₃S₁₁ precursors prepared using ACN, THP, and Dox solvents. An endothermic peak was observed between 100 and 200 °C, which is attributed to the evaporation of the solvent coordinated with lithium thiophosphates. Differential thermal analysis showed that the strength of the chemical interaction between the Li₂S-P₂S₅ system and solvent molecules increased with an increasing dielectric permittivity of the coordinated solvent. Therefore, the correlation between the conductivity and dielectric permittivity can be described using the argument that the use of an organic solvent with high dielectronic permittivity increases the reactivity of the precursor, resulting in the formation of the highly pure Li₇P₃S₁₁. Besides dielectronic permittivity, other selection criteria for the suspension synthesis of Li₂S-P₂S₅ systems include the absence of side reactions with raw materials, intermediates, and products, as well as a reasonably low boiling point. Given these requirements, ACN solvent is the optimal choice for the suspension synthesis of Li₇P₃S₁₁ at present.

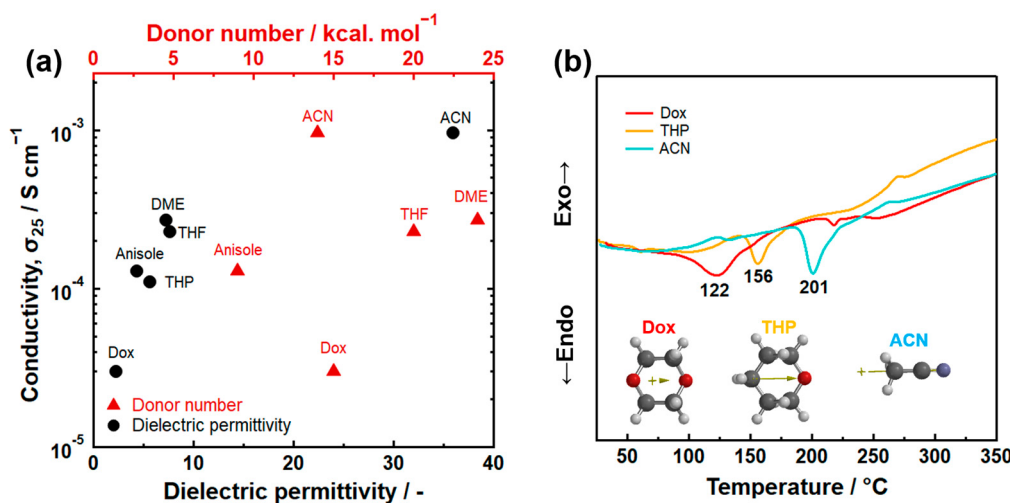


Figure 3. (a) The relationship between the dielectric permittivity of organic solvents and ionic conductivity at room temperature of Li₇P₃S₁₁ prepared by the suspension synthesis method. Dox represents 1,4-dioxane and THP represents tetrahydropyran. (b) Differential thermal curves of Li₇P₃S₁₁ precursors prepared using ACN, THP, and Dox solvents [15]. The arrows within the molecular structure represent dipole moment.

3.3. Solubility

The formation of soluble precursors is preferred for the reaction to proceed quickly. EA solvent completely dissolves the intermediate resulting from 70Li₂S 30P₂S₅, enabling the rapid synthesis of Li₇P₃S₁₁ SEs [21]. Individual Li₂S and P₂S₅ are insoluble in EA solvent during solution synthesis. This indicates that a rapid synthesis for sulfide SEs does

not necessarily require the solubilization of Li_2S and P_2S_5 raw material. In other words, the overall reaction rate in the synthesis process depends on the solubility of solvents for intermediate complexes, as follows: ACN and EP dissolve $1\text{Li}_2\text{S} 1\text{P}_2\text{S}_5$ (molar ratio) [24,28]; THF dissolves $1.5\text{Li}_2\text{S} 1\text{P}_2\text{S}_5$ [52]; and a mixed solvent of ACN and THF at a volume ratio of 1:1 dissolves $2\text{Li}_2\text{S} 1\text{P}_2\text{S}_5$ [53]. Of course, the solubility of the solvent depends on a given compound. The solubility of $\text{Li}_2\text{S}-\text{GeS}_2$ and $\text{Li}_2\text{S}-\text{SnS}_2$ in organic solvents remains poorly understood. The strong covalent bonding between the metal and chalcogen atoms typically brings a challenge for the direct dissolution of these compounds. In 2009, it was reported that a bulk chalcogenide semiconductor and chalcogen in hydrazine solvent form a highly soluble hydrazinium-based salt of the chalcogenide semiconductor through a redox reaction [54]. Hydrazine is an effective solvent for the solution processing of metal chalcogenide, but its highly toxic, explosive, and carcinogenic properties make it less attractive for scale-up. A binary thiol/amine mixture was developed as an ideal alkahest solvent system for the solution processing of chalcogenide semiconductors [55]. A mixed solvent of EDA and EDT fully dissolves SnS_2 and GeS_2 [49,56]. EDA solvents do not cause a nucleophilic attack to the germanium moiety on GeS_2 , even though EDA solvent with high DN shows a strong nucleophilic attacker capable of breaking P-S bonds. In contrast, the thiolate anion in thiol solvents dissociates Ge-S bonds in the GeS_2 through the nucleophilic attack. The high solubility of the mixed solvent of EDA and EDT for sulfides was first demonstrated in studies on the dissolution of bulk semiconductors, such as As_2Ch_3 , Sb_2Ch_3 , and Bi_2Ch_3 ($\text{Ch} = \text{S}, \text{Se}, \text{Te}$) which are insoluble in common organic solvents [57]. As mentioned above, depending on the solvent combination, mixed solvents may show higher solubility than a single solvent. Recent work reported that the mixtures of Li_2S and SiS_2 with a molar ratio of 2:1 are soluble in ACN solvent [58]. However, no comprehensive guidelines for gaining high solubility in starting materials for sulfide SEs have been proposed.

4. Strategies for Rapid Synthesis

4.1. Solubilizer

Solution synthesis is a desirable manufacturing technology for sulfide SEs. However, there are restrictions on the selection of solvents that dissolve raw materials and intermediates, e.g., Li_2S and Li_3PS_4 , and no leading guidelines for solvent selection have been established. The introduction of a solubilizer has been examined as one of the strategies to dissolve Li_2S and Li_3PS_4 . Excess elemental sulfur reacts with these insoluble materials to form intermediate molecular complexes that are soluble in specific solvents, such as THF and diethylene glycol diethyl ether (DEGDME) [59,60]. Lim et al. first proposed solution processing using excess elemental sulfur as the manufacturing technology for sulfide-based ASLBs [59]. In the sulfide SE solution processing, Li_2S and S reacted in DEGDME solvent to form fully soluble lithium polysulfides. Subsequently, P_2S_5 was added to the obtained solution to generate the $\beta\text{-Li}_3\text{PS}_4$ precursor. The $\beta\text{-Li}_3\text{PS}_4$ after drying treatment exhibited an ionic conductivity of $2.8 \times 10^{-5} \text{ S cm}^{-1}$ at room temperature. The low conductivity might be attributed to residual sulfur due to an insufficient drying process at 140°C . The synthesis method using excess sulfur requires a heat-treatment process over 250°C for the removal of excess sulfur, and is therefore unsuitable for synthesizing SEs that exhibit high ionic conductivity in the low-temperature phase, for example, amorphous Li_3PS_4 and $\text{Li}_7\text{P}_2\text{S}_8\text{I}$. Subsequent work successfully synthesized $\text{Li}_6\text{PS}_5\text{Cl}$ SEs via soluble lithium thiophosphates with excess sulfur, which showed a high ionic conductivity of 1.8 mS cm^{-1} at room temperature [61]. However, the reported solution processing via polysulfide involved a long reaction time of 24 h or more. To achieve rapid solution synthesis of $\text{Li}_7\text{P}_3\text{S}_{11}$, a synthesis method based on polysulfide chemistry was introduced (Figure 4a) [53]. Conventional suspension synthesis of highly conductive $\text{Li}_7\text{P}_3\text{S}_{11}$ requires a long reaction process to ensure sufficient reaction completion (Figure 4b). As shown in Figure 4c, the $7\text{Li}_2\text{S} 3\text{P}_2\text{S}_5$ system in ACN solvent formed a white suspension and a yellowish solution after stirring for 3 days; they correspond to the Li_3PS_4 complex and soluble

$1\text{Li}_2\text{S} \cdot 1\text{P}_2\text{S}_5$, respectively. According to the reaction mechanism proposed in the previous reports, $\text{Li}_7\text{P}_3\text{S}_{11}$ SEs are formed through a solid-state reaction of the Li_3PS_4 complex and $\text{Li}_2\text{S} \cdot \text{P}_2\text{S}_5$ (a molar ratio of 1:1) intermediate during heat treatment above 200 °C [29]. On the other hand, $7\text{Li}_2\text{S} \cdot 3\text{P}_2\text{S}_5 \cdot 5\text{S}$ in a mixed solvent of ACN, THF, and a trace amount of EtOH formed a black colored solution without additional energy in an extremely short time of 2 min (Figure 4d). The formation of the black solution suggests the presence of polysulfide ions. In the UV-Vis absorption spectra of $7\text{Li}_2\text{S} \cdot 3\text{P}_2\text{S}_5 \cdot 5\text{S}$ in the mixed solvent, S_8 , S_6^{2-} , S_4^{2-} , and S_3^{2-} were detected at 265, 350, 410, and 610 nm, respectively (see Figure 4e). Research in the field of lithium sulfur batteries reported that lithium polysulfides with different chain lengths are stabilized in specific organic solvents through disproportionate and dissociation reactions [62,63]. Tri-sulfur radical anions with high reactivity are the dominant chemical species in the complex system of equilibria. The reaction kinetics in the synthesis method with excess sulfur is significantly influenced by the chemical stability of the S_3^{2-} radical anions. Intrinsically unstable S_3^{2-} radical anions are stabilized in highly polar organic solvents because of the competition for Li ions between strong coordinated bonds of highly polar solvents and electrostatic interactions of polysulfide anions. The rapid solution synthesis shown in Figure 4a can be achieved by the existence of highly polar EtOH, which enhances the chemical stability of the S_3^{2-} radical anion in the precursor solution.

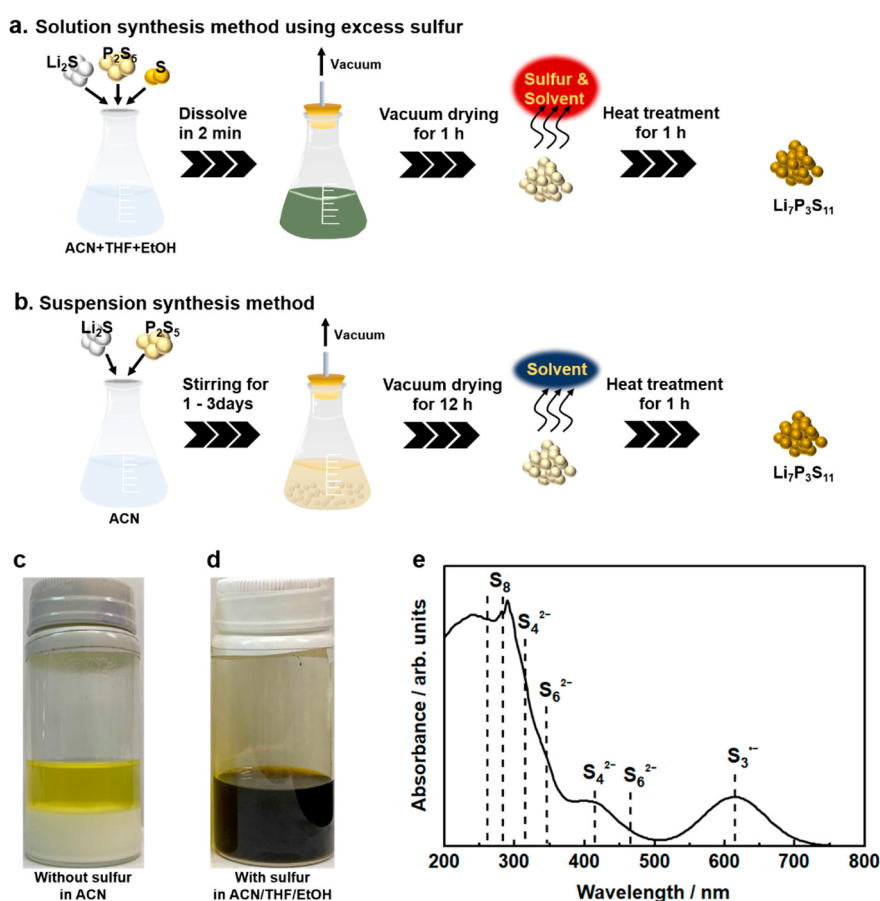


Figure 4. Schematics of (a) the solution synthesis method using excess sulfur and (b) the suspension synthesis method for $\text{Li}_7\text{P}_3\text{S}_{11}$ SEs. Solubility of (c) $7\text{Li}_2\text{S} \cdot 3\text{P}_2\text{S}_5$ mixtures in ACN solvent after stirring at 50 °C for 72 h and (d) $7\text{Li}_2\text{S} \cdot 3\text{P}_2\text{S}_5 \cdot 5\text{S}$ in ACN/THF/EtOH solvent after stirring at room temperature for 2 min. (e) UV-Vis spectrum of $7\text{Li}_2\text{S} \cdot 3\text{P}_2\text{S}_5 \cdot 5\text{S}$ at 1.0 mmol L⁻¹ in ACN/THF/EtOH solvent [53].

Figure 5 outlines the proposed reaction of lithium phosphates with excess elemental sulfur in the precursor solution [53]. First, lithium ions form strong coordination bonds with highly polar EtOH and ACN solvents (step 1). Next, the polysulfides generated by the reaction of Li_2S and excess sulfur are shielded from Li ions (Step 2). Tri-sulfur radical anions are stabilized owing to the competition between the polysulfide dianions and salt anions for the Li cation (Step 3). Then, the $\text{S}_3^{\cdot-}$ radical anions with unpaired electrons attack the phosphorus moiety on P_4S_{10} (step 4). The P_4S_{10} with an adamantane-like cage structure dissociates to reactive P_2S_5 (step 5). The reactive P_2S_5 reacts with lithium polysulfides to form a soluble lithium thiophosphate. The added excess elemental sulfur is removed without deteriorating influence on the formation of the final products during the heat treatment for crystallization. Recent works demonstrated that $\text{Li}_6\text{PS}_5\text{Cl}$ and $\text{Li}_{10}\text{GeP}_2\text{S}_{12}$ are rapidly synthesized via the precursor solution with excess elemental sulfur in the ACN/THF/EtOH solvent [64,65]. A mixture of Li_2S , P_2S_5 , LiX ($\text{X} = \text{Cl}, \text{Br}$, and I), and S at a molar ratio of 5:1:2:15, which represents the raw materials of $\text{Li}_6\text{PS}_5\text{X}$ SEs, formed a black solution in the ACN/THF/EtOH solvent, as shown in Figure 6a. This black coloration arises from the formation of polysulfide ions (see Figure 6b–d). The existence of a trace EtOH enhanced the solubility of the precursor solution and the chemical stability of polysulfides, which is explained by the coordination chemistry shown in Figure 5.

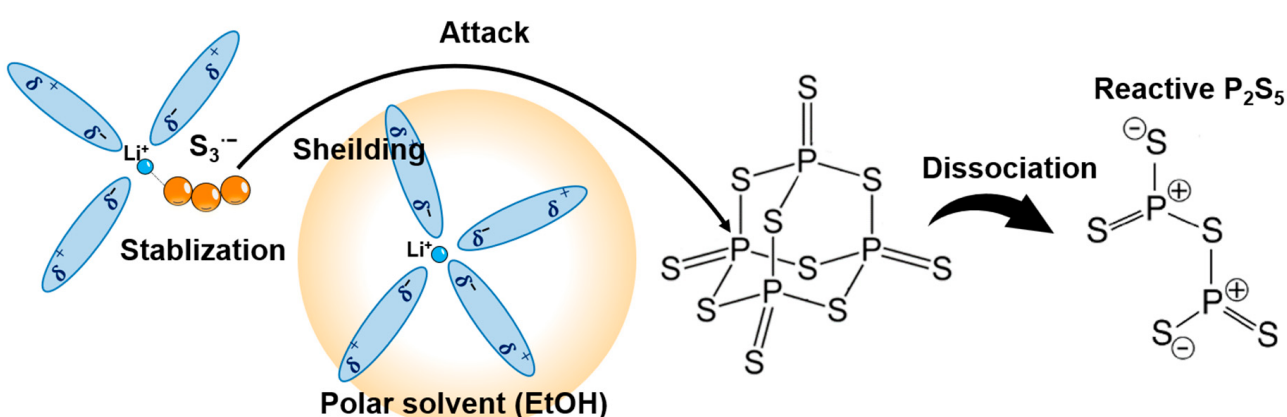


Figure 5. Schematics of the reaction mechanism for $\text{Li}_2\text{S}\text{-P}_2\text{S}_5$ systems in ACN/THF/EtOH solvent [53]. Step 1: Lithium ions are strongly coordinated with highly polar EtOH molecules. Step 2: Polysulfides are shielded from Li ions. Step 3: $\text{S}_3^{\cdot-}$ radical anions are stabilized. Step 4: The S radical anions attack the phosphorus moiety on P_4S_{10} . Step 5: P_4S_{10} with cage structure breaks and converts to reactive P_2S_5 .

Interestingly, $5\text{Li}_2\text{S} \text{ } 2\text{LiCl} \text{ } 15\text{S}$ precursor in ACN/THF solvent formed a reddish-brown solution, indicating lower chemical stability of the polysulfides than other precursor solutions. A Raman study showed that this observation may be caused by the strong competitive interaction between Cl ions and ACN molecules in the precursor solution [64]. In this solution synthesis method using excess elemental sulfur as a solubilizer, the coordination environment of solvent molecules, Li-ions, and polysulfides determines the chemical stability and reactivity of each chemical species. The coordination chemistry is also of interest in the research field of lithium-sulfur batteries [63,66,67]. Thus, this method can promise further advances by integrating the insight gained from coordination chemistry studies in the field of lithium-sulfur batteries.

4.2. Reactant Agent

As mentioned above, the wet-chemical synthesis of lithium thiophosphates initiates the dissociation reaction of P_4S_{10} . The dissociation reaction is driven by nucleophilic attack from lone-pair electrons of Li_2S and/or donor solvents [26,29]. The introduction of reactant agents for activating P_4S_{10} is a useful strategy for the rapid synthesis of sulfide SEs. The

addition of lithium thioethoxide and lithium halide facilitates the formation of soluble chemical species [64,68,69]. Halide ions are nucleophilic, and quickly dissociate P_2S_5 in organic solvents, as shown in Figure 6e [64]. Lithium ions are strongly solvated by donor solvents owing to their strong Lewis acid. Therefore, the bond of Li ions with counter ions is strongly polarized and more easily dissociated. In the coordination environment, where the cation is highly stabilized, the anion species would be available as reactive chemical species in the system. Taking this into consideration, the reaction mechanism in the wet-chemical synthesis of $Li_7P_2S_8I$ SEs may intrinsically differ from that of Li_3PS_4 [23,24].

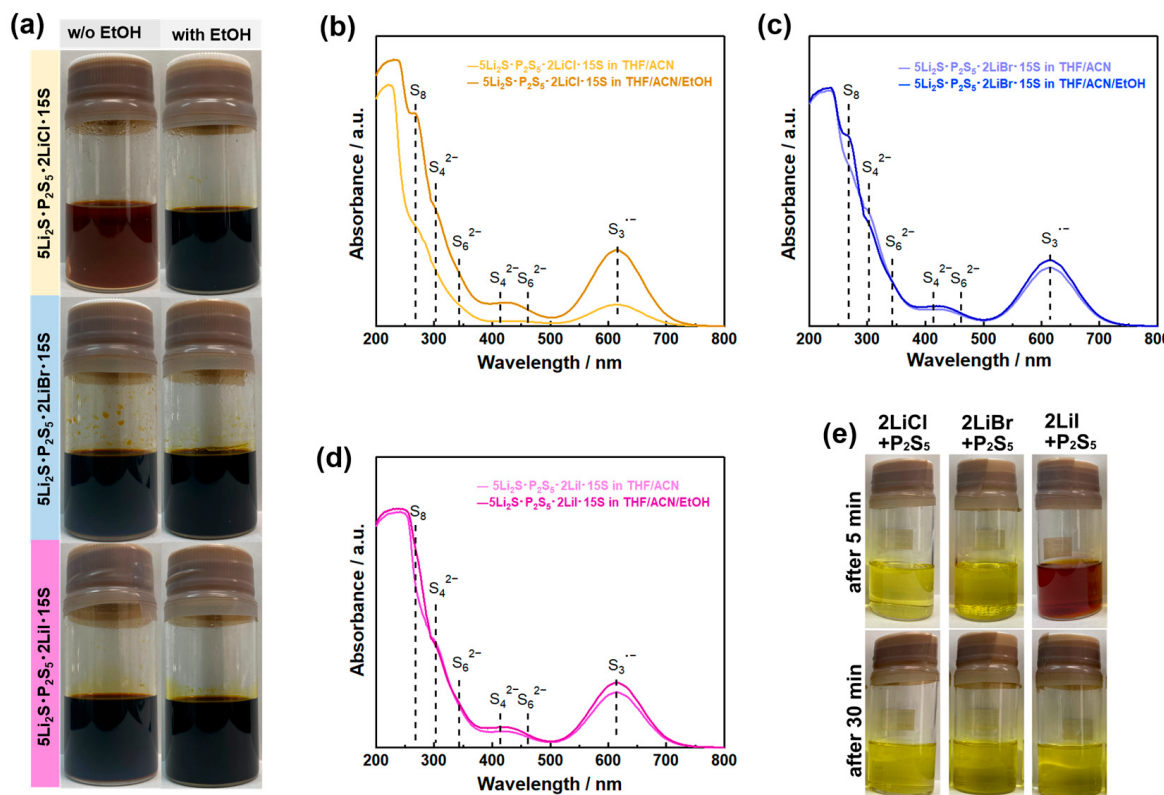


Figure 6. (a) Optical images of $5\text{Li}_2\text{S}\text{P}_2\text{S}_5\text{15S}$ (molar ratio) and $5\text{Li}_2\text{S}\text{P}_2\text{S}_5\text{2LiX 15S}$ ($\text{X} = \text{Cl}, \text{Br}$, and I) at 0.1 mol L^{-1} in ACN/THF and $\text{ACN}/\text{THF}/\text{EtOH}$ solvents. UV-Vis spectra of (b) $5\text{Li}_2\text{S}\text{P}_2\text{S}_5\text{2LiCl 15S}$, (c) $5\text{Li}_2\text{S}\text{P}_2\text{S}_5\text{2LiBr 15S}$, and (d) $5\text{Li}_2\text{S}\text{P}_2\text{S}_5\text{2LiI 15S}$ solutions at 0.5 mmol L^{-1} in ACN/THF and $\text{ACN}/\text{THF}/\text{EtOH}$ solvents. (e) Optical images of $2\text{LiCl}\cdot\text{P}_2\text{S}_5$, $2\text{LiCl}\cdot\text{P}_2\text{S}_5$, and $2\text{LiCl}\cdot\text{P}_2\text{S}_5$ in THF/ACN solvent (0.1 mol L^{-1}) from the standing samples for 5 and 30 min. Reprint with permission [63]; Copyright 2023, American Chemical Society.

5. Low-Cost Synthesis

The price of ASLBs per energy density is one order of magnitude higher than that of conventional LIBs, and is dominated by the cost of raw materials for SEs [61]. Among these raw materials, Li_2S , an essential raw material, is one to two orders of magnitude more cost-expensive per gram than P_2S_5 [12]. Hence, it is necessary to develop a synthetic method using inexpensive starting materials instead of Li_2S . A liquid-phase synthesis of Li-ion SEs using inexpensive Na_2S raw material was recently developed: the synthesis of Li_4SnS_4 from Na_4SnS_4 using the ion-exchange method [70]; and the synthesis of $\text{Li}_6\text{PS}_5\text{Cl}$ using Na_2S as a sulfurizing agent [71–73].

5.1. Ion-Exchange Method

Li_4SnS_4 was synthesized from Na_4SnS_4 using the ion-exchange method via water [70]. Firstly, an Na_4SnS_4 solution was prepared through the reaction between Na_2S and SnS_2 in water. The obtained Na_4SnS_4 solution flowed through a column packed with Li-type ion

exchange resin to exchange from Na^+ to Li^+ ions in Na_4SnS_4 . The resultant Li_4SnS_4 aqueous solution was dried and heated to obtain Li_4SnS_4 SEs (see Figure 7). The Li_4SnS_4 obtained from this method showed an ionic conductivity of approximately $1 \times 10^{-4} \text{ S cm}^{-1}$ at room temperature, which is the same value as Li_4SnS_4 prepared by the solid-phase method and mechanochemical reaction. Unlike Li_2S , Na_2S can be handled in air, and it is easy to process the reaction in an aqueous solution. This method using inexpensive Na_2S and H_2O as reaction solvents resolves environmental loads owing to the use of organic solvents and economic concerns.

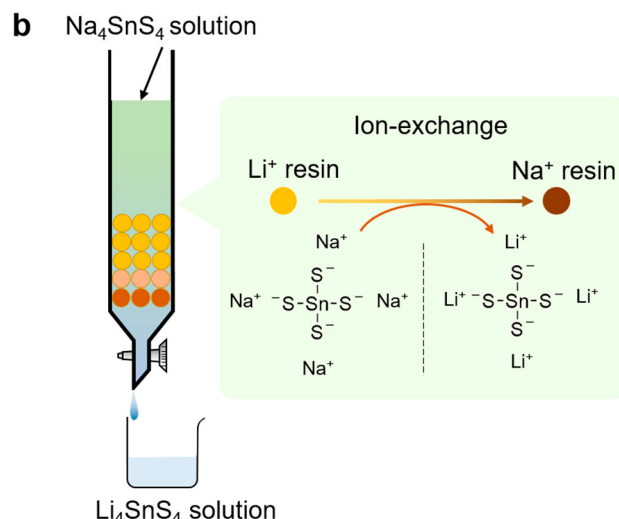
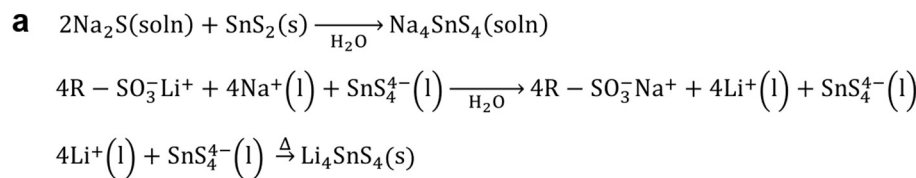
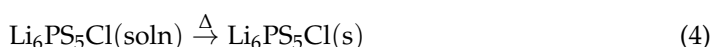
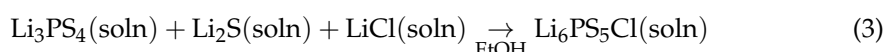
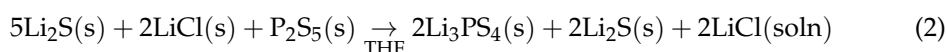
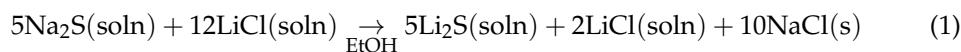


Figure 7. (a) Reactions and (b) schematic for the synthesis of Li_4SnS_4 solid electrolytes via aqueous solution ion-exchange. The circles in the schematic represent ion exchange resin.

5.2. Sulfurizing Agent

Lithium chloride reacts with Na_2S in EtOH solvent to generate precipitated Na_2S and $\text{Li}_2\text{S}/\text{LiCl}$ EtOH solution [71–74]. The $\text{Li}_2\text{S}/\text{LiCl}$ mixture powder, separated by the distillation of the product, and P_2S_5 are added into THF solvent to form Li_3PS_4 intermediate molecular complexes. The Li_3PS_4 , Li_2S , and LiCl mixture powder, prepared by the drying treatment of the precursor suspension, dissolves in EtOH solvent, followed by drying and heat treatment to obtain $\text{Li}_6\text{PS}_5\text{Cl}$ SEs.



This method allows us to synthesize Li_2S from Na_2S and LiCl on the basis of the difference in the solubility of EtOH for Li_2S and NaCl . A further examination of the

sulfurizing agent such as Na_2S can contribute to the development of the liquid-phase synthesis for sulfide SEs from inexpensive Li salts other than Li_2S .

6. Environmental Aspects

The industrial adaption of the liquid-phase synthesis for sulfide SEs to the electric vehicle fields requires consideration of environmental aspects, such as the toxicity of sulfide SEs and organic solvents, yield rate, energy-saving route, recycling of sulfide SEs. Sulfide SEs consisting of P or Si element release toxic gas, that is, H_2S gas, in contact with atmospheric moisture [75–77]. The air-stability of these materials is based on the classical hard-soft acid-base theory (HSAB) [76–81]. According to HSAB theory, the sulfur anion is a softer base than the oxygen anion and thus metal cations classified as softer acids form stronger bonds with sulfur than oxygen. Using softer acids, such as Sn^{4+} and Sb^{5+} , as central cations has been an effective strategy to improve the air stability of sulfide SEs. Importantly, Li_4SnS_4 can be processed in a solution using water, which is the most environmentally friendly solvent [78]. This stability is desirable for recycling technology of sulfide SEs through energy-saving routes. Indeed, the Li_4SnS_4 subjected to exposure to water, followed by vacuum drying and heat treatment, showed almost the same ionic conductivity as the as-synthesized Li_4SnS_4 [78]. However, a family of Li_4SnS_4 SEs showed an ionic conductivity in the order of 10^{-4} S cm^{-1} at room temperature, which is insufficient for practical application in ASLBs [70,78–80]. On the other hand, the solution processing of a family of $\text{Li}_2\text{S}-\text{P}_2\text{S}_5$ with high ionic conductivity in water is unable to avoid detrimental effects on the electrochemical and structural properties of the $\text{Li}_2\text{S}-\text{P}_2\text{S}_5$ SEs [75]. The use of green solvent EtOH in solution processing may potentially contribute to the environmentally friendly synthesis of sulfide SEs [39,42,71,72]. In some cases, the introduction of protective agents may be necessary. The influence of green solvents on the nature of sulfide SEs still requires further exploration [82,83]. Such a chemical perspective would offer significant insights into SE recycling.

7. Summary

In this review, we have highlighted a chemical perspective on the liquid-phase synthesis of sulfide SEs for ASLBs. This article has discussed the role of an additive (e.g., reactant, solubilizer, and sulfurizing agent) and organic solvent for realizing rapid and low-cost synthesis of sulfide SEs.

The liquid-phase synthesis method of sulfide solid electrolytes for all-solid-state batteries offers many advantages: low cost, high scalability, and short processing time. The liquid-phase synthesis method is classified into the suspension method and solution method. The chemical reaction in these methods is determined by the nature of the solvent. We summarized a guideline for solvent selection based on the donor number, dielectric permittivity, and solubility. The suspension method leads to low energy consumption during solvent removal; however, it involves a long processing time owing to the poor reaction kinetics in the precursor suspension. In contrast, the solution method provides higher scalability and a shorter processing time than the suspension method. Studies on the solvent effect induced by various solvent combinations have the potential to greatly advance large-scale solution synthesis technologies. Moreover, the addition of the solubilizer and reactant is an effective strategy for achieving enhanced reaction kinetics in wet-chemical synthesis. The addition of excess elemental sulfur plays a role as the solubilizer and reactant, offering the rapid solution synthesis of a variety of SEs. Given that the cost of ASLBs is still higher than conventional LIBs, the development of a synthesis method using inexpensive raw materials instead of Li_2S reduces barriers to the commercialization of ASLBs. Additionally, minimizing solvent removal in the synthesis process will increase the feasibility of its application into all-solid-state battery manufacturing. The chemical perspective in the liquid-phase synthesis gives significant insight into recycling SEs. The recent progress in the community of ASLBs has focused on their demonstration in lab-scale

cells. There is a demand for the development of a large-scale manufacturing technology that takes into account environmental load owing to the use of organic solvent and cost.

Author Contributions: Conceptualization, H.G.; writing—original draft preparation, H.G.; writing—review and editing, A.N. and A.M.; visualization, H.G. All authors have read and agreed to the published version of the manuscript.

Funding: This research received no funding.

Data Availability Statement: No new data were created or analyzed in this study. Data sharing is not applicable to this article.

Conflicts of Interest: The authors declare no conflict of interest.

References

1. Larcher, D.; Tarascon, J.-M. Towards greener and more sustainable batteries for electrical energy storage. *Nat. Chem.* **2015**, *7*, 19–29. [[CrossRef](#)] [[PubMed](#)]
2. Cano, Z.P.; Banham, D.; Ye, S.; Hintennach, A.; Lu, J.; Fowler, M.; Chen, Z. Batteries and fuel cells for emerging electric vehicle markets. *Nat. Energy* **2018**, *3*, 279–289. [[CrossRef](#)]
3. Lim, H.-D.; Park, J.-H.; Shin, H.-J.; Jeong, J.; Kim, J.T.; Nam, K.-W.; Jung, H.-G.; Chung, K.Y. A review of challenges and issues concerning interfaces for all-solid-state batteries. *Energy Storage Mater.* **2020**, *25*, 224–250. [[CrossRef](#)]
4. Zhang, Q.; Cao, D.; Ma, Y.; Natan, A.; Aurora, P.; Zhu, H. Sulfide-Based Solid-State Electrolytes: Synthesis, Stability, and Potential for All-Solid-State Batteries. *Adv. Mater.* **2019**, *31*, 1901131–1901172. [[CrossRef](#)]
5. Yamane, H.; Shibata, M.; Shimane, Y.; Junke, T.; Seino, Y.; Adams, S.; Minami, K.; Hayashi, A.; Tatsumisago, M. Crystal structure of a superionic conductor, Li₇P₃S₁₁. *Solid State Ion.* **2007**, *178*, 1163–1167. [[CrossRef](#)]
6. Kamaya, N.; Hommna, K.; Yamakawa, Y.; Hirayama, M.; Kannno, R.; Yonemura, M.; Kamiyama, T.; Kato, Y.; Hama, S.; Kawamoto, K.; et al. A lithium superionic conductor. *Nat. Mater.* **2011**, *10*, 682–686. [[CrossRef](#)]
7. Takada, K. Progress and prospective of solid-state lithium batteries. *Acta Mater.* **2013**, *61*, 759–770. [[CrossRef](#)]
8. Manthiram, A.; Yu, X.; Wang, S. Lithium battery chemistries enabled by solid-state electrolytes. *Nat. Rev. Mater.* **2017**, *2*, 16103–16118. [[CrossRef](#)]
9. Lee, J.; Lee, T.; Char, K.; Kim, K.J.; Choi, W.J. Issues and Advances in Scaling up Sulfide-Based All-Solid-State Batteries. *Acc. Chem. Res.* **2021**, *54*, 3390–3402. [[CrossRef](#)]
10. Miura, A.; Rosero-Navarro, N.C.; Sakuda, A.; Tadanaga, K.; Phuc, N.H.H.; Matsuda, A.; Machida, N.; Hayashi, A.; Tatsumisago, M. Liquid-phase syntheses of sulfide electrolytes for all-solid-state lithium battery. *Nat. Rev. Chem.* **2019**, *3*, 189–198. [[CrossRef](#)]
11. Gamo, H. Development of All-Solid-State Batteries with Sulfide Solid Electrolytes. Ph.D. Thesis, Toyohashi University of Technology, Toyohashi, Japan, 2023.
12. Ghidiu, M.; Ruhl, J.; Culver, S.P.; Zeier, W.G. Solution-based synthesis of lithium thiophosphate superionic conductors for solid-state batteries: A chemistry perspective. *J. Mater. Chem. A* **2019**, *7*, 17735–17753. [[CrossRef](#)]
13. Gutmann, V. Solvent effects on the reactivities of organometallic compounds. *Coord. Chem. Rev.* **1976**, *18*, 225–255. [[CrossRef](#)]
14. Calpa, M.; Nakajima, H.; Mori, S.; Goto, Y.; Mizuguchi, Y.; Moriyoshi, C.; Kuroiwa, Y.; Rosero-Navarro, N.C.; Miura, A.; Tadanaga, K. Formation Mechanism of β-Li₃PS₄ through Decomposition of Complexes. *Inorg. Chem.* **2021**, *60*, 6964–6970. [[CrossRef](#)]
15. Gamo, H.; Nagai, A.; Matsuda, A. The effect of solvent on reactivity of the Li₂S–P₂S₅ system in liquid-phase synthesis of Li₇P₃S₁₁ solid electrolyte. *Sci. Rep.* **2021**, *11*, 21097–21104. [[CrossRef](#)] [[PubMed](#)]
16. Xu, R.C.; Xia, X.H.; Yao, Z.J.; Wang, X.L.; Gu, C.D.; Tu, J.P. Preparation of Li₇P₃S₁₁ glass-ceramic electrolyte by dissolution–evaporation method for all-solid-state lithium ion batteries. *Electrochim. Acta* **2016**, *219*, 235–240. [[CrossRef](#)]
17. Wang, X.; Ye, L.; Nan, C.W.; Li, X. Effect of Solvents on a Li₁₀GeP₂S₁₂-Based Composite Electrolyte via Solution Method for Solid-State Battery Applications. *ACS Appl. Mater. Interfaces* **2022**, *14*, 46627–46634. [[CrossRef](#)]
18. Yamamoto, M.; Terauchi, Y.; Sakuda, A.; Takahashi, M. Binder-free sheet-type all-solid-state batteries with enhanced rate capabilities and high energy densities. *Sci. Rep.* **2018**, *8*, 1212–1221. [[CrossRef](#)]
19. Liu, Z.; Fu, W.; Payzant, A.; Yu, X.; Wu, Z.; Dudney, N.J.; Kiggans, J.; Hong, K.; Rondinone, A.J.; Liang, C. Anomalous high ionic conductivity of nanoporous β-Li₃PS₄. *J. Am. Chem. Soc.* **2013**, *135*, 975–978. [[CrossRef](#)]
20. Ito, S.; Nakakita, M.; Aihara, Y.; Uehara, T.; Machida, N. A synthesis of crystalline Li₇P₃S₁₁ solid electrolyte from 1,2-dimethoxyethane solvent. *J. Power Sources* **2014**, *271*, 342–345. [[CrossRef](#)]
21. Zhou, J.; Chen, Y.; Yu, Z.; Bowden, M.; Miller, Q.R.S.; Chen, P.; Scharf, H.T.; Mueller, K.T.; Lu, D.; Xiao, J.; et al. Wet-chemical synthesis of Li₇P₃S₁₁ with tailored particle size for solid state electrolytes. *Chem. Eng. J.* **2022**, *429*, 132334. [[CrossRef](#)]
22. Yamamoto, K.; Yang, S.; Takahashi, M.; Ohara, K.; Uchiyama, T.; Watanabe, T.; Sakuda, A.; Hayashi, A.; Tatsumisago, M.; Muto, H.; et al. High Ionic Conductivity of Liquid-Phase-Synthesized Li₃PS₄ Solid Electrolyte, Comparable to That Obtained via Ball Milling. *ACS Appl. Energy Mater.* **2021**, *4*, 2275–2281. [[CrossRef](#)]
23. Phuc, N.H.H.; Hirahara, E.; Morikawa, K.; Muto, H.; Matsuda, A. One-pot liquid phase synthesis of (100-x)Li₃PS₄-xLiI solid electrolytes. *J. Power Sources* **2017**, *365*, 7–11. [[CrossRef](#)]

24. Phuc, N.H.H.; Morikawa, K.; Totani, M.; Muto, H.; Matsuda, A. Chemical synthesis of Li_3PS_4 precursor suspension by liquid-phase shaking. *Solid State Ion.* **2016**, *285*, 2–5. [[CrossRef](#)]
25. Rajagopal, R.; Subramanian, Y.; Jung, Y.J.; Kang, S.; Ryu, K.-S. Rapid Synthesis of Highly Conductive $\text{Li}_6\text{PS}_5\text{Cl}$ Argyrodite-Type Solid Electrolytes Using Pyridine Solvent. *ACS Appl. Energy Mater.* **2022**, *5*, 9266–9272. [[CrossRef](#)]
26. Ghidiu, M.; Schlem, R.; Zeier, W.G. Pyridine Complexes as Tailored Precursors for Rapid Synthesis of Thiophosphate Superionic Conductors. *Batteries Supercaps* **2021**, *4*, 607–611. [[CrossRef](#)]
27. Maniwa, R.; Calpa, M.; Rosero-Navarro, N.C.; Miura, A.; Tadanaga, K. Synthesis of sulfide solid electrolytes from Li_2S and P_2S_5 in anisole. *J. Mater. Chem. A* **2021**, *9*, 400–405. [[CrossRef](#)]
28. Matsuda, A.; Muto, H.; Phuc, N.H.H. Preparation of Li_3PS_4 Solid Electrolyte by Liquid-Phase Shaking Using Organic Solvents with Carbonyl Group as Complex Forming Medium. *J. Jpn. Soc. Powder Powder Metall.* **2016**, *63*, 976–980. [[CrossRef](#)]
29. Shi, J.; Liu, G.; Weng, W.; Cai, L.; Zhang, Q.; Wu, J.; Xu, X.; Yao, X. $\text{Co}_3\text{S}_4@\text{Li}_7\text{P}_3\text{S}_{11}$ Hexagonal Platelets as Cathodes with Superior Interfacial Contact for All-Solid-State Lithium Batteries. *ACS Appl. Mater. Interfaces* **2020**, *12*, 14079–14086. [[CrossRef](#)]
30. Calpa, M.; Rosero-Navarro, N.C.; Miura, A.; Tadanaga, K. Instantaneous preparation of high lithium-ion conducting sulfide solid electrolyte $\text{Li}_7\text{P}_3\text{S}_{11}$ by a liquid phase process. *RSC Adv.* **2017**, *7*, 46499–46504. [[CrossRef](#)]
31. Rangasamy, E.; Liu, Z.; Gobet, M.; Pilar, K.; Sahu, G.; Zhou, W.; Wu, H.; Greenbaum, S.; Liang, C. An Iodide-Based $\text{Li}_7\text{P}_2\text{S}_8\text{I}$ Superionic Conductor. *J. Am. Chem. Soc.* **2015**, *137*, 1384–1387. [[CrossRef](#)]
32. Hikima, K.; Yamamoto, T.; Phuc, N.H.H.; Matsuda, R.; Muto, H.; Matsuda, A. Improved ionic conductivity of $\text{Li}_2\text{S}-\text{P}_2\text{S}_5-\text{LiI}$ solid electrolytes synthesized by liquid-phase synthesis. *Solid State Ion.* **2020**, *354*, 115403–115408. [[CrossRef](#)]
33. Zhou, L.; Park, K.-H.; Sun, X.; Lalere, F.; Adermann, T.; Hartmann, P.; Nazar, L.F. Solvent-Engineered Design of Argyrodite $\text{Li}_6\text{PS}_5\text{X}$ ($\text{X} = \text{Cl}, \text{Br}, \text{I}$) Solid Electrolytes with High Ionic Conductivity. *ACS Energy Lett.* **2019**, *4*, 265–270. [[CrossRef](#)]
34. Indrawan, R.F.; Gamo, H.; Nagai, A.; Matsuda, A. Chemically Understanding the Liquid-Phase Synthesis of Argyrodite Solid Electrolyte $\text{Li}_6\text{PS}_5\text{Cl}$ with the Highest Ionic Conductivity for All-Solid-State Batteries. *Chem. Mater.* **2023**, *35*, 2549–2558. [[CrossRef](#)]
35. Calpa, M.; Rosero-Navarro, N.C.; Miura, A.; Terai, K.; Utsuno, F.; Tadanaga, K. Formation mechanism of thiophosphate anions in the liquid-phase synthesis of sulfide solid electrolytes using polar aprotic solvents. *Chem. Mater.* **2020**, *32*, 9627–9632. [[CrossRef](#)]
36. Wang, Y.; Lu, D.; Bowden, M.; Khouri, P.Z.E.; Han, K.S.; Deng, Z.D.; Xiao, J.; Zhang, J.-G.; Liu, J. Mechanism of Formation of $\text{Li}_7\text{P}_3\text{S}_{11}$ Solid Electrolytes through Liquid Phase Synthesis. *Chem. Mater.* **2018**, *30*, 990–997. [[CrossRef](#)]
37. Wang, Z.; Jiang, Y.; Wu, J.; Jiang, Y.; Hung, S.; Zhao, B.; Chen, Z.; Zhang, J. Reaction mechanism of $\text{Li}_2\text{S}-\text{P}_2\text{S}_5$ system in acetonitrile based on wet chemical synthesis of $\text{Li}_7\text{P}_3\text{S}_{11}$ solid electrolyte. *Chem. Eng. J.* **2020**, *393*, 124706–124714. [[CrossRef](#)]
38. Tsukasaki, H.; Mori, S.; Shiotani, S.; Yamamura, H. Ionic conductivity and crystallization process in the $\text{Li}_2\text{S}-\text{P}_2\text{S}_5$ glass electrolyte. *Solid State Ion.* **2018**, *317*, 122–126. [[CrossRef](#)]
39. Yubuchi, S.; Uematsu, M.; Hotehama, C.; Sakuda, A.; Hayashi, A.; Tatsumisago, M. An argyrodite sulfide-based superionic conductor synthesized by a liquid-phase technique with tetrahydrofuran and ethanol. *J. Mater. Chem. A* **2019**, *7*, 558–566. [[CrossRef](#)]
40. Ruhl, J.; Riegger, L.M.; Ghidiu, M.; Zeier, W.G. Impact of Solvent Treatment of the Superionic Argyrodite $\text{Li}_6\text{PS}_5\text{Cl}$ on Solid-State Battery Performance. *Adv. Energy Sustain. Res.* **2021**, *2*, 2000077–2000086. [[CrossRef](#)]
41. Song, Y.B.; Kim, D.H.; Kwak, H.; Han, D.; Kang, S.; Lee, J.H.; Bak, S.-M.; Nam, K.-W.; Lee, H.-W.; Jung, Y.S. Tailoring Solution-Processable Li Argyrodites $\text{Li}_{6+x}\text{P}_{1-x}\text{M}_x\text{S}_5\text{I}$ ($\text{M} = \text{Ge}, \text{Sn}$) and Their Microstructural Evolution Revealed by Cryo-TEM for All-Solid-State Batteries. *Nano Lett.* **2020**, *20*, 4337–4345. [[CrossRef](#)]
42. Yubuchi, S.; Uematsu, M.; Deguchi, M.; Hayashi, A.; Tatsumisago, M. Lithium-Ion-Conducting Argyrodite-Type $\text{Li}_6\text{PS}_5\text{X}$ ($\text{X} = \text{Cl}, \text{Br}, \text{I}$) Solid Electrolytes Prepared by a Liquid-Phase Technique Using Ethanol as a Solvent. *ACS Appl. Energy Mater.* **2018**, *1*, 3622–3629. [[CrossRef](#)]
43. Heo, Y.J.; Seo, S.D.; Hwang, S.H.; Choi, S.H.; Kim, D.W. One-pot aprotic solvent-enabled synthesis of superionic Li-argyrodite solid electrolyte. *Int. J. Energy Res.* **2022**, *46*, 17644–17653. [[CrossRef](#)]
44. Ito, A.; Kimura, T.; Sakuda, A.; Tatsumisago, M.; Hayashi, A. Liquid-phase synthesis of Li_3PS_4 solid electrolyte using ethylenediamine. *J. Sol-Gel Sci. Technol.* **2021**, *101*, 2–7. [[CrossRef](#)]
45. Kimura, T.; Ito, A.; Nakano, T.; Hotehama, C.; Kowada, H.; Sakuda, A.; Tatsumisago, M.; Hayashi, A. Crystalline precursor derived from Li_3PS_4 and ethylenediamine for ionic conductors. *J. Sol-Gel Sci. Technol.* **2022**, *104*, 627–634. [[CrossRef](#)]
46. Teragawa, S.; Aso, K.; Tadanaga, K.; Hayashi, A.; Tatsumisago, M. Liquid-phase synthesis of a Li_3PS_4 solid electrolyte using N-methylformamide for all-solid-state lithium batteries. *J. Mater. Chem. A* **2014**, *2*, 5095–5099. [[CrossRef](#)]
47. Tan, D.H.S.; Banerjee, A.; Deng, Z.; Wu, E.A.; Nguyen, H.; Douz, J.-M.; Wang, X.; Cheng, J.-h.; Ong, S.P.; Meng, Y.S.; et al. Enabling Thin and Flexible Solid-State Composite Electrolytes by the Scalable Solution Process. *ACS Appl. Energy Mater.* **2019**, *2*, 6542–6550. [[CrossRef](#)]
48. Woo, J.; Song, Y.B.; Kwak, H.; Jun, S.; Jang, B.Y.; Park, J.; Kim, K.T.; Park, C.; Lee, C.; Park, K.-H.; et al. Liquid-Phase Synthesis of Highly Deformable and Air-Stable Sn-Substituted Li_3PS_4 for All-Solid-State Batteries Fabricated and Operated under Low Pressures. *Adv. Energy Mater.* **2023**, *13*, 2203292. [[CrossRef](#)]
49. Lee, J.E.; Park, K.-H.; Kim, J.C.; Wi, T.-U.; Ha, A.R.; Song, Y.B.; Oh, D.Y.; Woo, J.; Kweon, S.H.; Yeom, S.J.; et al. Universal Solution Synthesis of Sulfide Solid Electrolytes Using Alkahest for All-Solid-State Batteries. *Adv. Mater.* **2022**, *34*, 2200083–2200093. [[CrossRef](#)]

50. Ozturk, T.; Ertas, E.; Mert, O. A berzelius reagent, phosphorus decasulfide (P_4S_{10}), in organic syntheses. *Chem. Rev.* **2010**, *110*, 3419–3478. [[CrossRef](#)]
51. Gutmann, V. Empirical parameters for donor and accepter properties of solvents. *Electrochim. Acta* **1976**, *21*, 661–670. [[CrossRef](#)]
52. Fan, B.; Xu, Y.; Ma, R.; Luo, Z.; Wang, F.; Zhang, X.; Ma, H.; Fan, P.; Xue, B.; Han, W. Will Sulfide Electrolytes be Suitable Candidates for Constructing a Stable Solid/Liquid Electrolyte Interface? *ACS Appl. Mater. Interfaces* **2020**, *12*, 52845–52856. [[CrossRef](#)] [[PubMed](#)]
53. Gamo, H.; Nishida, J.; Nagai, A.; Hikima, K.; Matsuda, A. Solution Processing via Dynamic Sulfide Radical Anions for Sulfide Solid Electrolytes. *Adv. Energy Sustain. Res.* **2022**, *3*, 2200019–2200027. [[CrossRef](#)]
54. Yuan, M.; Mitzi, D.B. Solvent properties of hydrazine in the preparation of metal chalcogenide bulk materials and films. *Dalton Trans.* **2009**, *31*, 6078–6088. [[CrossRef](#)] [[PubMed](#)]
55. McCarthy, C.L.; Brutney, R.L. Solution processing of chalcogenide materials using thiol–amine ‘alkahest’ solvent systems. *Chem. Commun.* **2017**, *53*, 4888–4902. [[CrossRef](#)] [[PubMed](#)]
56. Antunez, P.D.; Torelli, D.A.; Yang, F.; Rabuffetti, F.A.; Lewis, N.S.; Brutney, R.L. Low Temperature Solution-Phase Deposition of SnS Thin Films. *Chem. Mater.* **2014**, *26*, 5444–5446. [[CrossRef](#)]
57. Webber, D.H.; Brutney, R.L. Alkahest for V_2VI_3 Chalcogenides: Dissolution of Nine Bulk Semiconductors in a Diamine-Dithiol Solvent Mixture. *J. Am. Chem. Soc.* **2013**, *135*, 15722–15725. [[CrossRef](#)]
58. Ito, T.; Hori, S.; Hirayama, M.; Kanno, R. Liquid-phase synthesis of the $Li_{10}GeP_2S_{12}$ -type phase in the Li-Si-P-S-Cl system. *J. Mater. Chem. A* **2022**, *10*, 14392–14398. [[CrossRef](#)]
59. Lim, H.; Lim, H.-K.; Xing, X.; Lee, B.-S.; Liu, H.; Coaty, C.; Kim, H.; Liu, P. Solid Electrolyte Layers by Solution Deposition. *Adv. Mater. Interfaces* **2018**, *5*, 1701328–1701336. [[CrossRef](#)]
60. Li, Y.; Wang, X.; Zhou, H.; Xing, X.; Banerjee, A.; Holoubek, J.; Liu, H.; Meng, Y.S.; Liu, P. Thin Solid Electrolyte Layers Enabled by Nanoscopic Polymer Binding. *ACS Energy Lett.* **2020**, *5*, 955–961. [[CrossRef](#)]
61. Kim, M.J.; Choi, I.-H.; Jo, S.C.; Kim, B.G.; Ha, Y.-C.; Lee, S.-M.; Kang, S.; Baeg, K.-J.; Park, J.-W. A Novel Strategy to Overcome the Hurdle for Commercial All-Solid-State Batteries via Low-Cost Synthesis of Sulfide Solid Electrolytes. *Small Methods* **2021**, *5*, 2100793–2100804. [[CrossRef](#)]
62. Bieker, G.; Wellmann, J.; Kolek, M.; Jalkanen, K.; Winter, M.; Bieker, P. Influence of cations in lithium and magnesium polysulphide solutions: Dependence of the solvent chemistry. *Phys. Chem. Chem. Phys.* **2017**, *19*, 11152–11162. [[CrossRef](#)] [[PubMed](#)]
63. Zhong, N.; Lei, C.; Meng, R.; Li, J.; He, X.; Liang, X. Electrolyte Solvation Chemistry for the Solution of High-Donor-Number Solvent for Stable Li-S Batteries. *Small* **2022**, *18*, 2200046–2200054. [[CrossRef](#)] [[PubMed](#)]
64. Gamo, H.; Kusaba, I.; Hikima, K.; Matsuda, A. Rapid Solution Synthesis of Argyrodite-Type Li_6PS_5X (X = Cl, Br, and I) Solid Electrolytes Using Excess Sulfur. *Inorg. Chem.* **2023**, *62*, 6076–6083. [[CrossRef](#)] [[PubMed](#)]
65. Hikima, K.; Ogawa, K.; Gamo, H.; Matsuda, A. $Li_{10}GeP_2S_{12}$ solid electrolytes synthesised via liquid-phase methods. *Chem. Commun.* **2023**, *43*, 6564–6567. [[CrossRef](#)]
66. Cuisinier, M.; Hart, C.; Balasubramanian, M.; Garsuch, A.; Nazar, L.F. Radical or Not Radical: Revisiting Lithium-Sulfur Electrochemistry in Nonaqueous Electrolytes. *Adv. Energy Mater.* **2015**, *5*, 1401801–1401806. [[CrossRef](#)]
67. Cuisinier, M.; Cabelguen, P.-E.; Adams, B.D.; Garsuch, A.; Balasubramanian, M.; Nazar, L.F. Unique behaviour of nonsolvents for polysulphides in lithium–sulphur batteries. *Energy Environ. Sci.* **2014**, *7*, 2697–2705. [[CrossRef](#)]
68. Lim, H.-D.; Yue, X.; Xing, X.; Petrova, V.; Gonzalez, M.; Liu, H.; Liu, P. Designing solution chemistries for the low-temperature synthesis of sulfide-based solid electrolytes. *J. Mater. Chem. A* **2018**, *6*, 7370–7374. [[CrossRef](#)]
69. Phuc, N.H.H.; Yamamoto, T.; Muto, H.; Matsuda, A. Fast synthesis of $Li_2S\text{-}P_2S_5\text{-}LiI$ solid electrolyte precursors. *Inorg. Chem. Front.* **2017**, *4*, 1660–1664. [[CrossRef](#)]
70. Matsuda, R.; Kokubo, T.; Phuc, N.H.H.; Muto, H.; Matsuda, A. Preparation of ambient air-stable electrolyte Li_4SnS_4 by aqueous ion-exchange process. *Solid State Ion.* **2020**, *345*, 115190. [[CrossRef](#)]
71. Han, A.; Tian, R.; Fang, L.; Wan, F.; Hu, X.; Zhao, Z.; Tu, F.; Song, D.; Zhang, X.; Yang, Y. A Low-Cost Liquid-Phase Method of Synthesizing High-Performance Li_6PS_5Cl Solid-Electrolyte. *ACS Appl. Mater. Interfaces* **2022**, *14*, 30824–30838. [[CrossRef](#)]
72. Smith, W.H.; Vaselabadi, S.A.; Wolden, C.A. Argyrodite Superionic Conductors Fabricated from Metathesis-Derived Li_2S . *ACS Appl. Energy Mater.* **2022**, *5*, 4029–4035. [[CrossRef](#)]
73. Smith, W.H.; Vaselabadi, S.A.; Wolden, C.A. Synthesis of high-purity Li_2S nanocrystals via metathesis for solid-state electrolyte applications. *J. Mater. Chem. A* **2023**, *11*, 7652–7661. [[CrossRef](#)]
74. Smith, W.H.; Vaselabadi, S.A.; Wolden, C.A. Sustainable synthesis of SiS_2 for solid-state electrolytes by cascaded metathesis. *Mater. Today Commun.* **2023**, *35*, 105574. [[CrossRef](#)]
75. Muramatsu, H.; Hayashi, A.; Ohtomo, T.; Hama, S.; Tatsumisago, M. Structural change of $Li_2S\text{-}P_2S_5$ sulfide solid electrolytes in the atmosphere. *Solid State Ion.* **2011**, *182*, 116–119. [[CrossRef](#)]
76. Otoyama, M.; Kuratani, K.; Kobayashi, H. A systematic study on structure, ionic conductivity, and air-stability of $xLi_4SnS_4\text{-(}1-x\text{)}Li_3PS_4$ solid electrolytes. *Ceram. Int.* **2021**, *47*, 28377–28383. [[CrossRef](#)]
77. Kimura, T.; Kato, A.; Hotehama, C.; Sakuda, A.; Hayashi, A.; Tatsumisago, M. Preparation and characterization of lithium ion conductive Li_3SbS_4 glass and glass-ceramic electrolytes. *Solid State Ion.* **2019**, *333*, 45–49. [[CrossRef](#)]
78. Park, K.H.; Oh, D.Y.; Choi, Y.E.; Nam, Y.J.; Han, L.; Kim, J.-Y.; Xin, H.; Lin, F.; Oh, S.M.; Jung, Y.S. Solution-Processable Glass $LiI\text{-}Li_4SnS_4$ Superionic Conductors for All-Solid-State Li-Ion Batteries. *Adv. Mater.* **2016**, *28*, 1874–1883. [[CrossRef](#)]

79. Zhao, F.; Liang, J.; Yu, C.; Sun, Q.; Li, X.; Adair, K.; Wang, C.; Zhao, Y.; Zhang, S.; Li, W.; et al. A Versatile Sn-Substituted Argyrodite Sulfide Electrolyte for All-Solid-State Li Metal Batteries. *Adv. Energy Mater.* **2020**, *10*, 1903422–1903431. [[CrossRef](#)]
80. Otoyama, M.; Kuratani, K.; Kobayashi, H. Mechanochemical synthesis of air-stable hexagonal Li_4SnS_4 -based solid electrolytes containing LiI and Li_3PS_4 . *RSC Adv.* **2021**, *11*, 38880–38888. [[CrossRef](#)]
81. Kimura, T.; Nakano, T.; Sakuda, A.; Tatsumisago, M.; Hayashi, A. Hydration and Dehydration Behavior of Li_4SnS_4 for Applications as a Moisture-Resistant All-Solid-State Battery Electrolyte. *J. Phys. Chem. C* **2023**, *127*, 1303–1309. [[CrossRef](#)]
82. Fang, L.; Zhang, Q.; Han, A.; Zhao, Z.; Hu, X.; Wan, F.; Yang, H.; Song, D.; Zhang, X.; Yang, Y. Green synthesis of the battery material lithium sulfide via metathetic reactions. *Chem. Commun.* **2022**, *58*, 5498–5501. [[CrossRef](#)] [[PubMed](#)]
83. Jo, Y.-S.; Hong, J.-W.; Choi, I.-H.; Sung, J.; Park, J.-H.; Park, H.; Kim, D.; Kim, B.G.; Ha, Y.-C.; Seo, J.; et al. Engineering green and sustainable solvents for scalable wet synthesis of sulfide electrolytes in high-energy-density all-solid-state batteries. *Green Chem.* **2023**, *25*, 1473–1487. [[CrossRef](#)]

Disclaimer/Publisher's Note: The statements, opinions and data contained in all publications are solely those of the individual author(s) and contributor(s) and not of MDPI and/or the editor(s). MDPI and/or the editor(s) disclaim responsibility for any injury to people or property resulting from any ideas, methods, instructions or products referred to in the content.